

Urea-induced unfolding of *Glossoscolex paulistus* hemoglobin, in oxy- and cyanomet-forms: A dissociation model

Francisco A.O. Carvalho^a, José Wilson P. Carvalho^a, Patrícia S. Santiago^{a,b}, Marcel Tabak^{a,*}

^a Instituto de Química de São Carlos, Universidade de São Paulo, SP, Brazil

^b Universidade Estadual Paulista "Julio de Mesquita Filho", Registro, São Paulo, SP, Brazil

ARTICLE INFO

Article history:

Received 30 July 2012

Received in revised form

22 September 2012

Accepted 25 September 2012

Available online 2 October 2012

Keywords:

Extracellular hemoglobin

HbGp

Urea

Oligomeric dissociation

AUC

SAXS

ABSTRACT

The urea effect on the giant extracellular hemoglobin of *Glossoscolex paulistus* (HbGp) stability was studied by analytical ultracentrifugation (AUC) and small angle X-ray scattering (SAXS). AUC data show that the sedimentation coefficient distributions curves $c(S)$, at 1.0 mol/L of urea, display a single peak at 57 S, associated to the undissociated protein. The increase in urea concentration, up to 4.0 mol/L, induces the appearance of smaller species, due to oligomeric dissociation. The sedimentation coefficients and molecular masses are 9.2 S and 204 kDa for the dodecamer $(abcd)_3$, 5.5 S and 69 kDa for the tetramer $(abcd)$, 4.1 S and 52 kDa for the trimer (abc) and 2.0 S and 17 kDa for the monomer d , respectively. SAXS data show initially a decrease in the $I(0)$ values due to the oligomeric dissociation, and then, above 4.0 mol/L of denaturant, for oxy-HbGp, and above 6.0 mol/L for cyanomet-HbGp, an increase in the maximum dimension and gyration radius is observed, due to the unfolding process. According to AUC and SAXS data the HbGp unfolding is described by two phases: the first one, at low urea concentration, below 4.0 mol/L, characterizes the oligomeric dissociation, while the second one, at higher urea concentration, is associated to the unfolding of dissociated species. Our results are complementary to a recent report based on spectroscopic observations.

© 2012 Elsevier B.V. Open access under the [Elsevier OA license](http://creativecommons.org/licenses/by/3.0/).

1. Introduction

Giant extracellular hemoglobins, also known as erythrocrurins, have been investigated as a model of extreme complexity in oxygen-binding heme proteins [1,2]. These extracellular hemoglobins are characterized by a very high molecular mass (MM), a high resistance to oxidation and a high oligomeric stability when subjected to conditions of stress such as high temperature, pH variation, and addition of chemical agents, such as urea and surfactants [3–6], as compared, for instance, with human hemoglobin. These properties make them an interesting and important system for investigation [2,7], including in biomedical applications. Besides, a strong motivation to study these giant hemoglobins is related to their potential use as blood substitutes. Studies have been performed in the past for *Lumbricus terrestris* hemoglobin (HbLt [8]), and are presently underway to test and validate the use of *Arenicola marina* hemoglobin (HbAm) in this direction [9,10]. They seem to be very promising due to the lack of undesirable immunological reactions in tests with animals, explained by the absence of cell membranes as occurs with human hemoglobin in red blood cells [9,10]. Besides, the resistance to oxidation of extracellular

hemoglobins, as noticed by their high redox stability, is also an advantage as compared to the use of human hemoglobin in this medical application.

The extracellular hemoglobin of *Glossoscolex paulistus* (HbGp) has a molecular mass of 3.6 MDa, determined recently by analytical ultracentrifugation (AUC, [11]). This protein has an oligomeric structure, similar to the orthologous HbLt [12], composed by 144 globin chains, and 36 additional chains lacking the heme group, named linkers. Mass spectrometry and AUC studies suggest that HbGp has the same stoichiometry as HbLt, based on the Vinogradov model, which assumes that the whole protein is composed by twelve protomers, constituted by a dodecamer of globin chains and a trimer of linkers, $[(abcd)_3L_3]$ [1,4,13]. Here a , b , c and d are globin chains forming an asymmetric tetramer $(abcd)$, composed of a disulfide bonded trimer (abc) and a monomeric subunit d . Three linker chains, L_1 , L_2 and L_3 complete the native protomer structure.

HbLt presents a high structural similarity as compared to HbGp, and the identity between the monomeric subunits d is 57%. The HbLt oxygenation process was investigated both for the whole oligomeric structure as well as for several structural parts of the protein in different conditions of pH, presence of salts and with the pure isolated subunits [14]. According to the authors, the tetramer $(abcd)$ has a high oxygen affinity, indistinguishable from the whole HbLt, at pH 6.8. However, the oxygen equilibrium of the trimer (abc) is characterized by a very low cooperativity and a maximum

* Corresponding author. Fax: +55 16 3373 9982.

E-mail address: marcel@sc.usp.br (M. Tabak).

Hill coefficient of 1.35 [14], significantly lower as compared to the whole protein, while the isolated subunits *a*, *b* and *c* do not present cooperativity in oxygen binding. Overall, these studies for HbLt suggest that $(abcd)_2$ is the primary cooperative unit in the oligomeric structure [14].

AUC studies of HbGp, at pH 10.0, show that the whole oligomer dissociates into monomer subunit *d*, dimer of monomers *d*, d_2 , trimer *abc*, and tetramer *abcd*. However, for cyanomet-HbGp, besides the appearance of these species, some fraction of undissociated whole protein is observed (17%), due to the fact that the cyanomet- form is more stable than oxy-HbGp, at pH 10.0 [4]. Spectroscopic studies of HbGp in the presence of urea suggested that urea induces, at low concentrations, between 1.0 and 3.0 mol/L, the oligomeric dissociation, and further increase in urea concentration promotes the denaturation of the dissociated species [6]. Cyanomet- and oxy-HbGp forms are more stable towards denaturation, in the presence of urea, than met-HbGp. Thus the order of stability in the presence of urea is given by: cyanomet- > oxy > met-HbGp [6].

Assuming a high similarity of the denaturation process for both oxy- and cyanomet-HbGp forms, described in the previous spectroscopic study, the focus of the present work is the characterization of the different species that exist in the solution, at different urea concentrations, and the evaluation of the global HbGp oligomeric dissociation model, in the presence of this denaturant agent. This study was performed using AUC and small angle X-ray scattering (SAXS). The additional SAXS and AUC data, obtained in this work, contribute to elucidate the species involvement and the oligomeric structure of this system and the differences between the unfolding processes of the oxy- and cyanomet-HbGp forms. Previous spectroscopic studies were able to give only a general view of the HbGp urea-induced unfolding, in three forms, and the species in the solution were not characterized.

2. Materials and methods

2.1. Protein extraction and purification

G. paulistus annelid is prevalent in sites near Piracicaba and Rio Claro cities in the state of São Paulo, Brazil. The HbGp was prepared using freshly drawn blood from the worms. HbGp solution was centrifuged at 2500 rpm for 15 min, at 4 °C. The sample was filtered (M_w cut-off 30 kDa) and centrifuged at $250,000 \times g$, at 4 °C, for 3 h. The pellet was resuspended in a minimum amount of 0.1 mol/L Tris-HCl buffer, at pH 7.0. Chromatography at pH 7.0 in a Sephadex G-200 column gave the samples used in the experiments [6,15–18]. All concentrations were determined spectrophotometrically in a UV-1601 PC spectrophotometer (Shimadzu, Japan), using the appropriate molar absorption coefficients [6,16]. The final protein concentration in our stock solution was in the range 15–40 mg/mL, in Tris-HCl 0.1 mol/L buffer, pH 7.0. To obtain the cyanomet-HbGp form, the met-HbGp was further incubated with a 5-fold molar excess of potassium cyanide relative to the heme. Excess of reagents was removed by dialysis against the same buffer for 3 h. The cyanomet-HbGp has a CN-ligand coordinated in the sixth coordination to the iron in the oxidized state (Fe^{3+}), while the oxy-HbGp has a molecule of O_2 as the sixth ligand with the iron in the reduced state (Fe^{2+}). All concentrations were determined spectrophotometrically using the absorption coefficients $\epsilon_{415nm} = 5.5 \pm 0.8 (\text{mg/mL})^{-1} \text{cm}^{-1}$ for oxy-HbGp and $\epsilon_{420nm} = 4.8 \pm 0.5 (\text{mg/mL})^{-1} \text{cm}^{-1}$ for cyanomet-HbGp [6,15].

2.2. AUC experiments

AUC experiments were performed in a Beckman Optima XL-A analytical ultracentrifuge. Sedimentation velocity (SV)

experiments were carried out at oxy-HbGp concentrations from 100 up to 300 $\mu\text{g/mL}$, in 100 mmol/L Tris-HCl, pH 7.0, containing 50 mmol/L NaCl. The samples were dialyzed against the same buffer, and the dialysate was used as reference solution in all experiments. The samples were exposed to 0.0–6.0 mol/L of urea 2 h before the experiments. In each unfolding titration experiment the appropriate volume of buffer and stock urea were mixed to achieve the desired urea concentration (0.0–6.0 mol/L) in a final volume of 1.0 mL, prior to the addition of a constant aliquot of concentrated protein solution, to give the desired final protein concentration. The urea concentration at 25 °C was estimated by the empirical formula suggested by Pace [19]:

$$[\text{Urea}] = 117.66(\Delta n) + 29.753(\Delta n)^2 + 185.56(\Delta n)^3 \quad (1)$$

where Δn is the difference between the refractive index of the urea solution and of the buffer.

The SV experiments were performed at 20 °C, using a rotor speed between 15,000 and 40,000 rpm (An60Ti rotor), and the scan data acquisition was measured at 236 and 416 nm. Absorbance data were collected using a radial step size of 0.003 cm. The sedimentation coefficient value is affected by temperature, viscosity (η) and density (ρ), so we calculated the standard sedimentation coefficient at infinite dilution (0 mg/mL, $s_{20,w}^0$). The Sednterp software was used to estimate the η and ρ values for each urea concentration [20,21]. The software SEDFIT (Version 12.52) [22,23] was applied in order to fit the absorbance versus cell radius raw data. This new version of software allows to estimate directly the values of $s_{20,w}$, presenting it as the *x*-axis in the *c* (*S*) distribution. The sedimentation coefficients ($s_{20,w}$) were found as the maximum of the peaks of the *c* (*S*) curves and the $s_{20,w}^0$ were estimated by linear regression of the $s_{20,w}$ values measured at each concentration.

Sedimentation equilibrium (SE) experiments were carried out for the oxy-HbGp at 5.0 mol/L of urea, at protein concentrations in the range 100–300 $\mu\text{g/mL}$, in 100 mmol/L Tris-HCl, pH 7.0, containing 50 mmol/L NaCl. The SE experiments were performed at 20 °C, using speeds of 15,000, 20,000 and 25,000 rpm with the An60Ti rotor, and the data were collected at 415 nm.

2.2.1. AUC data analysis

Sedimentation coefficient distribution function, *c* (*S*), was obtained by using SEDFIT program (Version 12.52) and the “Continuous *c* (*S*) Distribution” model. This software models the Lamm equation so as to discriminate the spreading of the sedimentation boundary from diffusion [22,23]. The *c* (*S*) distributions were obtained, keeping fixed the V_{bar} at 0.733 mL/g, and leaving the frictional ratio, f/f_0 , as the regularization parameter of the fitting process. The viscosity (η) and density (ρ) for each urea concentration were fixed. Besides, the distribution regularization method used was based on the “maximum entropy method” with a confidence interval $P=0.85$. The average value of rmsd in analyses of *c* (*S*) curves was 0.008 ± 0.002 , while the worst value found was 0.024.

The analyses of *MM* of the species present in solution in the SV experiments were made from the global fitting with the “Species Analysis” model of the SEDPHAT program (version 9.4). All parameters were allowed to float freely and then the statistical analyses were performed. The statistic method used was the “Monte-Carlo non-linear regression” with, at least, 200 iterations and a confidence level of 0.68.

The SE data analyses were also made globally with all samples (100, 200 and 300 $\mu\text{g/mL}$) and all speeds (15,000, 20,000 and 25,000 rpm), in the presence of 5.0 mol/L of urea, using the SEDPHAT program [24,25]. As initial input data, the *MM* determined by mass spectrometry [13] and the *s*-value determined by SV analysis [4] were used, and both parameters were allowed to float freely.

After the global fitting, statistical analyses were performed using the “Monte–Carlo non-linear regression” method provided by the SEDPHAT with, at least, 200 iterations, and the same confidence level of the SV experiments.

2.3. SAXS experiments

The protein concentrations used in these experiments were 0.5 and 3.0 mg/mL, in 30 mmol/L acetate–phosphate buffer, at pH 7.0, in the presence of urea, in the concentration range from 0.0 to 8.0 mol/L. Oxy-HbGp, cyanomet-HbGp, and pure buffer (in the absence and presence of different urea concentrations) were exposed for 90 s and the scattered X-rays intensity was monitored on an image plate detector. SAXS experiments were performed at the National Synchrotron Light Laboratory (LNLS), Campinas, Brazil, using a sample to detector distance of 731 mm and an X-ray wavelength, λ , of 1.608 Å. Scattering curves were recorded within the range 0.01–0.25 Å⁻¹. According to the sampling theorem [26], the maximum dimension of scattering particle that could be observed was circa 628 Å ($D_{\max} = 2\pi/q_{\min}$). The experimental intensities were corrected for sample attenuation, detector homogeneity, and blank scattering, both in the absence and in the presence of urea. The scattering vector amplitude q is defined as $q = 4\pi \sin \theta/\lambda$, 2θ being the scattering angle and λ the X-ray wavelength of 1.608 Å [26].

2.3.1. SAXS data analysis

Small angle X-ray scattering technique involves diffraction events from electrons and provides data about the protein structure at low resolution in solution [27,28]. In general, proteins are studied in high positive solute–solvent contrasts because they are more electron-dense than water and other buffer [27]. The scattering contributions associated to the presence of urea in solution were subtracted from the HbGp SAXS curves before the analysis. Therefore, it was necessary to measure a scattering curve for each solution containing the pure buffer and different experimental urea concentrations.

In this paper, the radius of gyration R_g , was determined by Guinier approximation [26] and using the GNOM software [29]. For a monodisperse solution of globular macromolecules the Guinier approximation is defined by Eq. (2) [26]:

$$I(q \rightarrow 0) = I(0) \exp^{-(R_g^2 q^2)/3} \quad (2)$$

Thus, $I(0)$ and R_g can be obtained from the y -axis intercept and the slope of the linear plot of $(\ln I(q))$ versus q^2 , respectively [26]. However, the range over which the Guinier approximation is valid for each measured scattering curve must be considered.

In the absence of interference effects, a Fourier transform connects the scattering intensity $I(q)$ to the pair distance distribution function, $p(r)$, which is related to the probability of finding a pair of small elements at a distance r within the entire volume of the scattering particle [26,30]. The $p(r)$ curve represents the structure in the real space and corresponds to the distribution of all the interatomic distances r within the macromolecule. In this work, we made use of the GNOM program [29] to obtain $p(r)$, R_g and D_{\max} values by fits of the experimental scattering curves.

Another important analysis in the study of denaturation of macromolecules by SAXS is the Kratky representation, which can be defined as the plot of $q^2 \cdot I(q)$ versus q [28,30]. Folded globular proteins have a prominent peak at low angles, whereas unfolded proteins display a continuous increase in $q^2 \cdot I(q)$ with q [28]. Thus, the Kratky representation is a good indicator of the protein structure in solution.

2.4. Dynamic light scattering (DLS) experiments

The instrument Zetasizer Nano ZS (Malvern, UK) was used on the light scattering measurements for particle size determination. This instrument allows dynamic light scattering measurements incorporating noninvasive backscattering (NIBS) optics. A He–Ne laser has been used as a light source with wavelength $\lambda = 633$ nm. The intensity of light scattered at an angle of 173° is measured by an avalanche photodiode. The solutions were placed in the thermostated sample chamber that maintained the sample stabilized at 25 °C, with an accuracy of 0.1 °C. At each sample seven measurements are performed and for each one a number of measurements is taken (normally around ten) to obtain an adequate statistics. The experiments were performed using oxy- and cyanomet-HbGp concentrations of 3.0 mg/mL at pH 7.0 in the phosphate 30 mmol/L buffer, in the urea concentration range from 0.0 to 8.0 mol/L. Samples were prepared following identical procedures as those used for SAXS. All DLS experiments were performed using a 45 μ L cuvette from Hellma (Hellma GmbH, Germany) with 3 mm \times 3 mm dimensions.

3. Results and discussions

3.1. AUC data

In Fig. 1 the $c(S)$ distributions are shown for oxy-HbGp in the presence of three urea concentrations. At 1.0 mol/L of urea, a single peak is observed, with sedimentation coefficient, $s_{20,w}$, around 57 S that can be assigned to the whole protein (Fig. 1A). In Table 1 the $s_{20,w}^0$ values are shown for all urea concentrations used in our experiments. This single $s_{20,w}^0$ value is consistent with the $s_{20,w}^0$ observed previously for oxy-HbGp, in the absence of urea, at pH 7.0 [11]. Moreover, other hydrodynamic properties, shown in Table 1, such as the MM of 3600 ± 100 kDa, and the Stokes radius (R_S) of 13.5 ± 0.2 nm, suggest that the species present at 1.0 mol/L of urea is indeed undissociated oxy-HbGp. The R_S value estimated for oxy-HbGp by AUC is very consistent with the hydrodynamic diameter value (D_h) of 27 ± 1 nm, determined independently by DLS studies [3]. The MM values shown in Table 1 were obtained by the global analysis of the sedimentation velocity data (SV) using the SEDPHAT software (version 9.4).

The increase of urea concentration induces the appearance of the contribution of other species in solution. At 2.0 mol/L of urea (Table 1) the contribution of two species is observed: the first one, with $s_{20,w}^0$ 10.3 ± 0.3 S and MM of 205 ± 5 kDa ($3 \pm 1\%$, Table 1), is associated to the dodecamer $(abcd)_3$ and the second species is assigned to the whole protein ($97 \pm 1\%$, Table 1). The R_S value found for the dodecamer varies between 6.2 and 5.1 nm (Table 1) and is consistent with the hydrodynamic diameter of 11 nm obtained by DLS experiments on the isolated dodecamer (data not shown). Our results suggest that oxy-HbGp is very stable at 2.0 mol/L of denaturant since the contribution of dissociated species in solution is quite small, reaching only 3%.

In this context, the work of Krebs et al. [31], focusing the properties of the dodecamer of HbL_t, has shown that this subunit obtained from urea-induced dissociation of the whole protein consisted of a concentration-dependent equilibrium of three species with sedimentation coefficients of 8.5–9.4 S, 3.6–4.4 S and 1.9 S. In a recent study of oxy- and cyanomet-HbGp forms, at pH 10.0 [4], no significant contribution of the dodecameric species $(abcd)_3$ in the solution was observed. This observation is, probably, due to a significant decrease of the HbGp stability in alkaline pH, above pH 9.0.

In Fig. 1B the $c(S)$ distributions are shown for oxy-HbGp, in the presence of 3.0 mol/L of urea, at pH 7.0, monitored at 415 nm. Three species appear in the distribution, where the smallest MM species is not observed at 1.0 and 2.0 mol/L of urea. This third species with

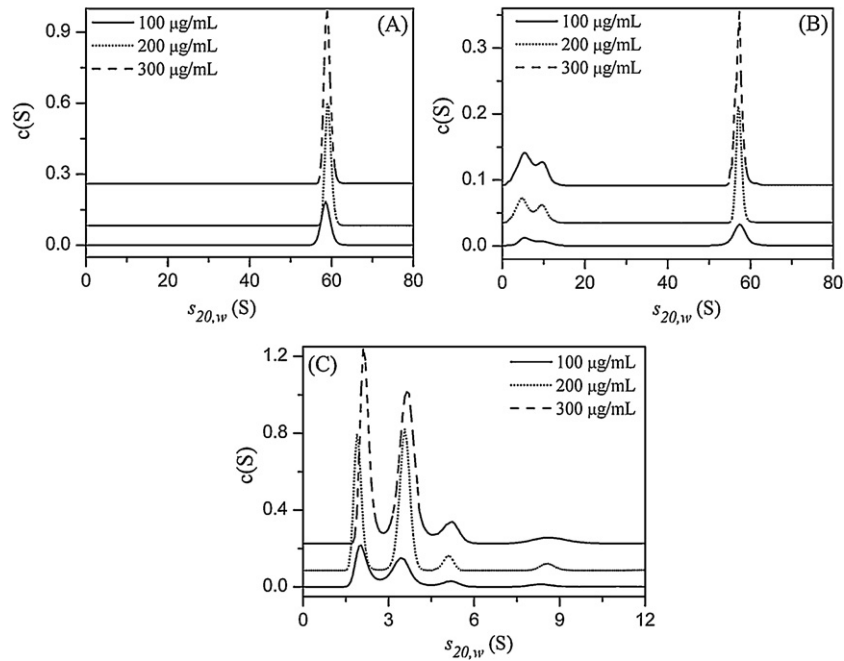


Fig. 1. Continuous sedimentation coefficient distributions of oxy-HbGp in 100 mmol/L Tris-HCl, pH 7.0, 50 mmol/L NaCl. The panel displays the $c(S)$ fittings for HbGp concentrations of 100, 200 and 300 $\mu\text{g/mL}$. The baselines for different protein concentrations are shifted along the ordinate axis to emphasize their differences. The $s_{20,w}^0$ for each concentration was determined as the maximum of Gaussian curves. Absorbance monitored at 415 nm. (A) Urea at 1.0 mol/L, (B) at 3.0 mol/L, and (C) at 6.0 mol/L.

Table 1

Hydrodynamic properties, $s_{20,w}^0$ in (S), MM in (kDa) and R_S in (nm), for the oxy-HbGp, in the presence of indicated urea concentrations, at pH 7.0 and 20 °C, obtained from sedimentation velocity (SV) data in the SEDFIT and SEDPHAT softwares. The Area corresponds to the species contribution (%) as measured by the corresponding area of $c(S)$ peaks.

[Urea] (mol/L)	Properties	Species observed				Whole protein
		Monomer, d	Trimer, abc	Tetramer, $abcd$	Dodecamer, $(abcd)_3$	
0.0	$s_{20,w}^0$	–	–	–	–	58.6 ± 0.6
	MM	–	–	–	–	3620 ± 80
	R_S	–	–	–	–	13.7 ± 0.1
	Area	–	–	–	–	100
1.0	$s_{20,w}^0$	–	–	–	–	57.3 ± 0.3
	MM	–	–	–	–	3600 ± 100
	R_S	–	–	–	–	13.5 ± 0.2
	Area	–	–	–	–	100
2.0	$s_{20,w}^0$	–	–	–	10.3 ± 0.3	57.3 ± 0.3
	MM	–	–	–	205 ± 5	3600 ± 100
	R_S	–	–	–	6.2 ± 0.3	13.3 ± 0.4
	Area	–	–	–	3 ± 1	97 ± 1
3.0	$s_{20,w}^0$	–	–	6.1 ± 0.8	9.2 ± 0.6	58.5 ± 0.6
	MM	–	–	72 ± 6	203 ± 16	3500 ± 200
	R_S	–	–	4.2 ± 0.3	6.1 ± 0.4	13.9 ± 0.3
	Area	–	–	20 ± 4	15 ± 2	65 ± 7
4.0	$s_{20,w}^0$	2.0 ± 0.6	3.8 ± 0.4	5.5 ± 0.4	9.4 ± 0.6	57.4 ± 0.6
	MM	17 ± 1	51 ± 1	70 ± 5	204 ± 3	3600 ± 50
	R_S	2.5 ± 0.2	3.2 ± 0.2	3.9 ± 0.3	5.1 ± 0.4	13.2 ± 0.2
	Area	25 ± 6	24 ± 5	8 ± 2	17 ± 6	26 ± 3
5.0	$s_{20,w}^0$	2.1 ± 0.6	4.1 ± 0.6	5.8 ± 0.5	9.3 ± 0.7	–
	MM	17 ± 2	53 ± 2	67 ± 4	202 ± 8	–
	MM^a	16.8 ± 0.7 ^a	52 ± 3 ^a	69 ± 2 ^a	206 ± 3 ^a	–
	R_S	2.4 ± 0.1	3.1 ± 0.2	3.8 ± 0.3	5.3 ± 0.6	–
6.0	$s_{20,w}^0$	2.1 ± 0.6	3.8 ± 0.5	5.3 ± 0.8	9.1 ± 0.8	–
	MM	18 ± 2	51 ± 4	71 ± 5	206 ± 12	–
	R_S	2.7 ± 0.5	3.5 ± 0.4	4.3 ± 0.2	5.5 ± 0.4	–
	Area	40 ± 2	49 ± 4	7 ± 1	4 ± 1	–
HbLt	$s_{20,w}^0$ ^b	1.83 ± 0.01	3.85 ± 0.02	4.73 ± 0.02	9.38 ± 0.05	–
	MM^c	16.6	53	69.6	208.8	3600

^a Molecular masses obtained by global fit of the equilibrium sedimentation data.

^b Prediction of the $s_{20,w}^0$ for the HbLt subunits by the HydroPro software [24].

^c Prediction of the MM for the HbLt subunits by the Sednterp software using the aminoacid sequence [9,20].

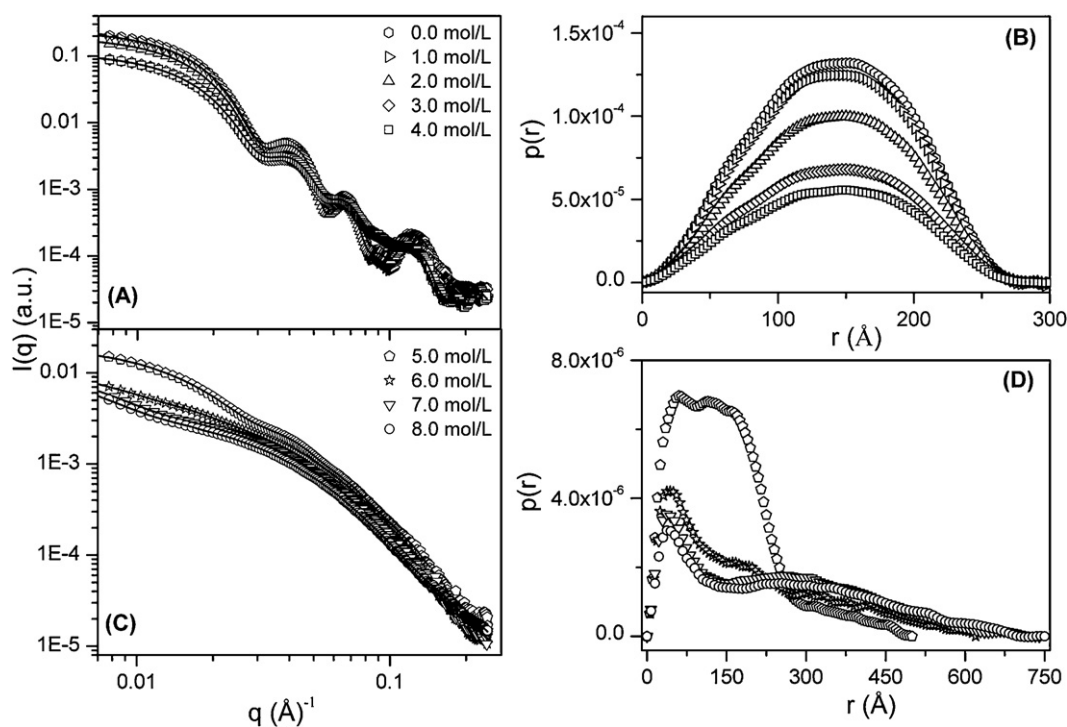


Fig. 2. (A) and (C) Small angle X-ray scattering curves of oxy-HbGp 3.0 mg/mL, in the 30 mmol/L acetate–phosphate buffer at pH 7.0, in the presence of urea. The symbols correspond to the experimental data and the lines to the fits by GNUM software. (B) and (D) Distance distribution functions $p(r)$ obtained from GNUM software corresponding to the scattering curves in the (A) and (C), respectively. The symbols shown in (B) and (D) have the same meaning as for (A) and (C).

$s_{20,w}^0$ of 6.1 ± 0.8 S and MM of 72 ± 6 kDa is assigned to the tetramer $abcd$ (Fig. 1B, Table 1). Furthermore, taking into account the limitations of the technique and the complexity of the samples, the values of MM for the tetramer ($abcd$) obtained from our SV data, by global analysis, are quite reasonable, as compared to the MM value of 68 kDa determined by MALDI-TOF-MS [13,32]. In Table 1 the relative percentages for the three species in equilibrium are displayed: they are, respectively, 20 ± 4 , 15 ± 2 and $65 \pm 7\%$, for the tetramer, dodecamer and whole protein. Therefore, the increase of urea concentration promotes the protein oligomeric dissociation, even though, the larger contribution of the solution species remains the whole protein ($65 \pm 7\%$), suggesting that, at 3.0 mol/L of urea, oxy-HbGp is still quite stable towards urea denaturation. Our results suggest that the dissociation process induced by urea is similar, in some aspects, to alkaline dissociation [4]. However, the urea-induced HbGp oligomeric dissociation, up to 4.0 mol/L of denaturant, is characterized by slight changes in the secondary structure, monitored in the peptide region, as well as, in the heme group region. Previous studies have shown that only slight alterations are observed in the ellipticity signal and in the Soret band absorbance [6]. Thus, the HbGp oligomeric dissociation induced by urea corresponds to the formation of an intermediate state in the unfolding process, quite similar to the native state.

At 4.0 mol/L of urea two additional new species are observed in equilibrium, as shown in Table 1. According to the sedimentation coefficient $s_{20,w}^0$ and molecular mass MM values, these new species can be attributed to the polypeptide chain d and the trimer abc . The values of $s_{20,w}^0$ and MM are 2.0 ± 0.6 S and 17 ± 1 kDa for the monomer d , and 3.8 ± 0.4 S and 51 ± 1 kDa for the trimer (abc), respectively (Table 1). The contribution of the undissociated protein decreases significantly to $26 \pm 3\%$, which is comparable to the contributions of the two dissociated species, the monomer and the trimer (around 25% each, Table 1). The sedimentation coefficients and MM values obtained for the monomer d and the trimer (abc) are similar to those found in our previous work [4,13,31]. Further increase of urea concentration, up to 5.0 mol/L,

leads to the complete protein dissociation into smaller species (Table 1). Percentage species contributions are 46 ± 2 , 37 ± 5 , 6 ± 1 and $11 \pm 4\%$, for the monomer d , trimer (abc), tetramer ($abcd$) and dodecamer ($abcd$)₃, respectively. The fact that, in the distributions curves, the contributions of the linker chains, L_1 , L_2 and L_3 are not observed, is, probably, due to the overlap of the contributions of these polypeptide chains with other species, being, for this reason, unresolved. In a recent paper, describing the characterization of HbGp species by SDS-PAGE electrophoresis and MALDI-TOF-MS, it is suggested that a linker chain is strongly bound to the trimer (abc) [32]. Besides, AUC measurements of isolated trimeric fractions show that 80% of the solution composition corresponds to the trimer (abc), and the remaining 20% are due to the trimer, associated to a linker chain ($abc+L$, data not shown, [32]).

The predictions of the $s_{20,w}^0$ for the linkers, based on the aminoacid sequences of the known HbLt chains, give values very close to the sedimentation coefficients obtained for the monomeric subunit d [32]. Thus, it is quite possible that the contributions from these polypeptide chains overlap with the contribution of the monomer d and trimer (abc) and, for this reason, the contribution of isolated linker chains is not observed. Besides, there are some additional points that make it difficult the characterization of the linkers in solution, such as their asymmetrical shape as compared to the globins chains, and their arrangement in the oligomeric structure, with a localization and orientation inside the oligomeric structure, more protected from the solvent. Our rigid body estimates for HbLt species suggest that the linkers, in the monomeric form, are expected to have hydrodynamic parameters close to those for our monomeric fraction, due to the high asymmetry of the linkers [32].

An initial analysis of SE data, for oxy-HbGp at pH 7.0, in the presence of 5.0 mol/L of urea, was performed by the SEDPHAT software using separate data sets corresponding to each individual protein concentration, but in a multi-speed mode. Based on these fits the MM for the species present in the solution were determined, and they are consistent with the data obtained by MALDI-TOF-MS [32], as well as, with the corresponding SV data (see Table 1).

Table 2SAXS and DLS parameters, for the extracellular hemoglobin of *G. paulistus*, in the oxy- and cyanomet- forms, at 3.0 mg/mL, in the presence of indicated urea concentrations.

HbGp forms	Urea (mol/L)	D_h (nm) ^a	PDI ^a	R_g (Å) ^b	R_g (Å) ^c	D_{max} (Å) ^b	$I(0)$ (a.u.) ^b
Oxy-	0.0	27 ± 1	0.002	106 ± 1	105 ± 10	300	0.26 ± 0.01
	2.0	29 ± 1	0.003	106 ± 1	107 ± 9	300	0.19 ± 0.01
	4.0	31 ± 1	0.035	106 ± 1	108 ± 8	300	0.10 ± 0.02
	5.0	30 ± 1	0.13	118 ± 2	115 ± 12	500	0.019 ± 0.005
	6.0	15 ± 1	0.25	169 ± 4	135 ± 17	620	0.012 ± 0.001
	7.0	14 ± 1	0.27	203 ± 6	201 ± 40	740	0.011 ± 0.001
Cyanomet-	0.0	27 ± 1	0.02	107 ± 1	107 ± 8	300	0.20 ± 0.01
	2.0	28 ± 1	0.005	106 ± 1	108 ± 7	300	0.16 ± 0.01
	4.0	31 ± 1	0.02	107 ± 1	107 ± 7	300	0.14 ± 0.02
	6.0	26 ± 1	0.23	106 ± 1	145 ± 20	350	0.034 ± 0.002
	7.0	14 ± 1	0.31	160 ± 2	166 ± 40	550	0.011 ± 0.001
	8.0	14 ± 1	0.32	189 ± 3	170 ± 30	600	0.009 ± 0.002

^a Parameters obtained by DLS experiments. D_h is the average hydrated diameter and PDI the polydispersity index.^b Parameters obtained by GNOM software. R_g is the radius of gyration, D_{max} the particle maximum dimension and $I(0)$ the scattering intensity at $q=0$.^c Radius of gyration obtained by Guinier approximation.

At 6.0 mol/L of urea (Fig. 1C), the observed species are, essentially, the same found at 5.0 mol/L. However, a significant decrease in the contribution of the dodecamer $(abcd)_3$ is observed, and the monomer d and the trimer (abc) are the predominant species, contributing both a total of 89% (Table 1). Thus, the increase of urea concentration induces further dissociation of the larger species in solution. At higher concentrations, urea induces the denaturation of the dissociated species, as monitored in a recent study by several spectroscopic techniques [6]. Differently from the studies at pH 10.0 [4], where the contribution of the dimer of monomers d , d_2 , with $s_{20,w}^0$ value around 2.7 S, was noticed, our results in the presence of urea suggest that this species is not observed.

3.2. SAXS and DLS data

Fig. 2 A and C shows the SAXS curves obtained for oxy-HbGp 3.0 mg/mL, at pH 7.0, 20 °C, as a function of the increase of urea concentration. SAXS curves, in the absence of urea, present three characteristics shoulders, centered at q values of 0.04 \AA^{-1} , 0.07 \AA^{-1} and 0.12 \AA^{-1} (see Fig. 2A). The corresponding distance distribution functions $p(r)$ and parameters obtained by GNOM software, for the oxy-HbGp, as a function of urea concentration, are shown in Fig. 2B and D, and in Table 2.

In the absence of urea, oxy-HbGp presents R_g , D_{max} and $I(0)$ values, respectively, of $106 \pm 1 \text{ \AA}$, 300 \AA , and 0.26 ± 0.01 , which are in agreement with previous SAXS studies [16]. In the presence of urea, in the range from 1.0 to 4.0 mol/L, no significant changes are observed in the values of D_{max} and R_g , characterizing the scattering particle dimensions (Table 2). However, a decrease in the scattering intensity at low q (Fig. 2A and C), $I(0)$, from 0.26 to 0.10 a.u. (Table 2) is noticed; this decrease and the $p(r)$ curves (Fig. 2B and D), suggest that oxy-HbGp undergoes partial dissociation, in this urea concentration range. The decrease of intensity is associated to the formation of smaller species in the solution, as observed in the AUC data (see Table 1). The changes in $p(r)$ curves and $I(0)$ values are relatively small due to the significant contribution of the whole protein scattering in this urea concentration range. Moreover, above 4.0 mol/L, the SAXS curves undergo significant changes: a dramatic decrease of $I(0)$, as well as, the loss in shoulders resolution are observed, suggesting the beginning of the denaturation process (Fig. 2A and C). Furthermore, at 5.0 mol/L of urea, increases of R_g from 106 ± 1 to $118 \pm 2 \text{ \AA}$ and D_{max} from 300 to 500 \AA are observed (Table 2). These changes, at 5.0 mol/L, can be associated to the oligomeric dissociation/denaturation process, as suggested in previous spectroscopic studies [6]. At 6.0 and 7.0 mol/L of urea, complete denaturation of HbGp species takes place, with R_g and D_{max} values of 169 ± 4 and $203 \pm 6 \text{ \AA}$, and 620 and 740 \AA , respectively (Table 2).

Therefore, above 4.0 mol/L, oxy-HbGp is extensively dissociated and denatured, as can be observed from the $p(r)$ profiles shown in Fig. 2B. The distance distribution function is characterized by a two-species population, one with smaller dimensions (R_g around 50 \AA) and a second one, characterized by a broad distribution with R_g values higher than 150 \AA . The smaller dimension species could be associated to the monomer and trimer species, while the species with higher dimensions could be assigned as the dodecamer, tetramer and one half of whole protein in denatured form, as observed in previous work [16].

Previous studies by optical absorption, fluorescence emission, and CD show that both forms, oxy- and cyanomet-HbGp have a similar denaturation process. However, the oxidized form displayed a higher stability. Thus, as the intermediate oligomers are the same for the two forms, only the SAXS study was made to compare the stability of the oxy- and cyanomet-HbGp forms.

The cyanomet-HbGp, in the presence of urea, has a similar dissociation and denaturation behavior as the oxy- form. However, cyanomet-HbGp is clearly more stable than the oxy- form, since it remains intact up to 5.0 mol/L of urea (see Fig. 3A). At 6.0 mol/L of denaturant, a decrease of $I(0)$ intensity occurs in the SAXS curves, as well as, the shoulders present a decrease of intensity and loss of resolution (Fig. 3C), consistent with the beginning of the oligomeric dissociation process [6]. The changes of the SAXS curves for cyanomet-HbGp are considerably smaller as compared with the oxy-form, at this urea concentration (see Fig. 2C and 3C). Moreover, for cyanomet-HbGp, the D_{max} values start to increase from 6.0 mol/L, while the R_g and $I(0)$ values already present some changes at lower urea concentrations. The R_g values, given by GNOM approximation, begin to increase at 7.0 mol/L of urea, from 106 ± 1 to $160 \pm 2 \text{ \AA}$. Furthermore, the $I(0)$ values show a 4-fold reduction (from 0.14 to 0.034 a.u.), probably, due to the oligomeric dissociation together with the beginning of the denaturation of the dissociated species in solution. However, the R_g values obtained by Guinier approximation, start to change significantly from 6.0 mol/L of urea, when an R_g increase from 107 ± 7 to $145 \pm 20 \text{ \AA}$ is observed (Table 2). Therefore, urea-induced cyanomet-HbGp unfolding, occurs between 6.0 and 7.0 mol/L, consistent with previous results based on spectroscopic studies [6]. The $p(r)$ distributions show that cyanomet-HbGp presents a similar behavior as oxy-HbGp, with significant changes shifted to higher urea concentrations (between 6.0 and 7.0 mol/L, Fig. 3D). The broader distribution of larger size species for cyanomet-HbGp suggests that, in this case, the oligomeric dissociation and denaturation processes, induced by urea, are more complex as compared to oxy-HbGp. This could be due to the higher resistance to unfolding of the whole protein and dissociated species of the oxidized form as compared to oxy-HbGp.

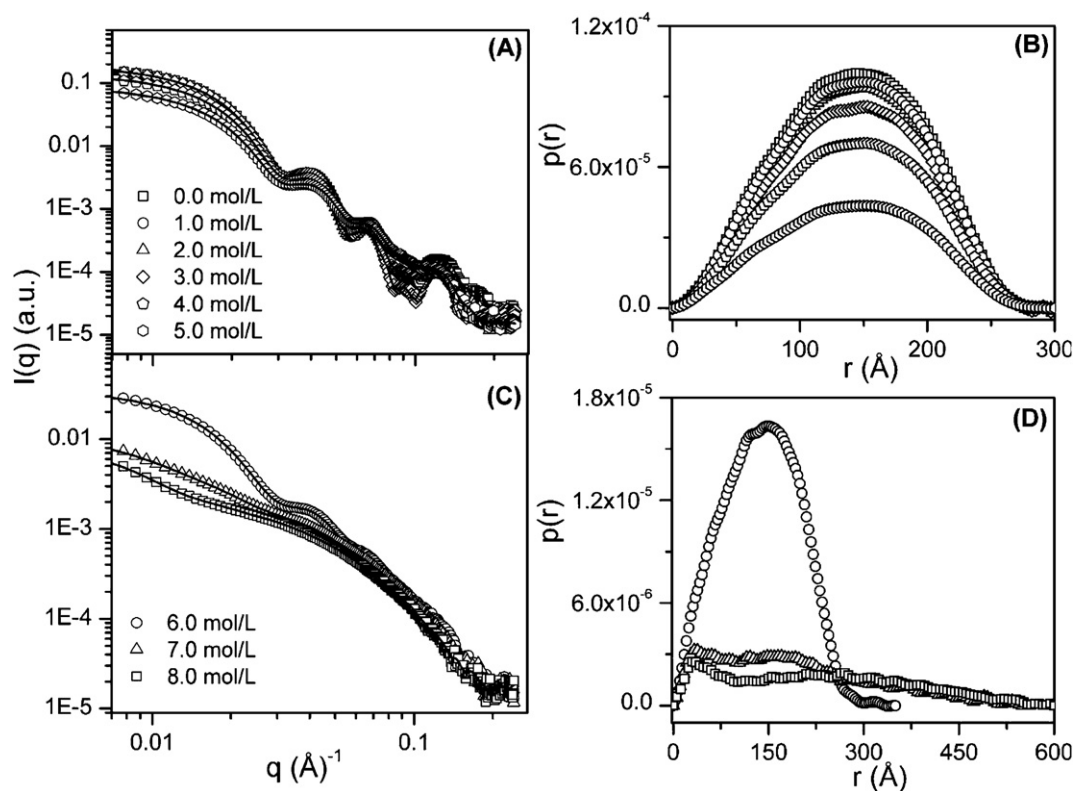


Fig. 3. (A) and (C) Small angle X-ray scattering curves of cyanomet-HbGp 3.0 mg/mL, in 30 mmol/L acetate–phosphate buffer at pH 7.0, in the presence of urea. The symbols correspond to the experimental data and the lines to the fits by GNOM software. (B) and (D) Distance distribution functions $p(r)$ obtained from GNOM software corresponding to the scattering curves in (A) and (C), respectively. The symbols shown in (B) and (D) have the same meaning as for (A) and (C).

Complementary studies were also performed for the urea-induced unfolding using a protein concentration of 0.5 mg/mL, for both oxy- and cyanomet-HbGp, at pH 7.0. At low protein concentration, the oxy- and cyanomet-HbGp are less stable in the presence of urea, since the two forms undergo changes above 3.0 and 4.0 mol/L of urea, respectively. As described above, at higher concentration, the changes on R_g , D_{max} and $I(0)$ parameters take place only above 4.0 mol/L and 6.0 mol/L, for both forms, respectively (Tables 2 and 3). The decrease of protein concentration, from 3.0 to 0.5 mg/mL promotes the oligomeric dissociation process earlier. Therefore, HbGp undergoes oligomeric dissociation at smaller urea concentrations (Tables 2 and 3). The effect of protein concentration in the dissociation process was observed previously by DLS and size exclusion chromatography [16]. AUC data were obtained for smaller protein concentrations, in the range from 100 to 300 $\mu\text{g/mL}$

and no significant differences in the $c(S)$ distributions were observed, probably, due to the small protein concentration range.

The corresponding Kratky's plots are shown in Fig. 4A and B. At 0.0 mol/L of urea, for oxy- and cyanomet-HbGp forms, characteristic peaks of folded globular proteins at low angles are observed, suggesting that the HbGp is totally folded. The increase in urea concentration induces a progressive peak intensity decrease, due to the oligomeric dissociation. Furthermore, at 5.0 and 7.0 mol/L of urea, for oxy- and cyanomet-HbGp, respectively, the complete peak disappearance is observed, indicating the protein denaturation.

Additional DLS experiments, performed for oxy- and cyanomet-HbGp, in the presence of urea, suggest that both oxidation forms are stable up to 4.0 mol/L, since the polydispersity index of the solution remains constant (Table 2), indicating mono-disperse

Table 3

R_g , D_{max} and $I(0)$ values for the extracellular hemoglobin of *G. paulistus*, in oxy- and cyanomet- forms at 0.5 mg/mL, in the presence of urea.

Urea (mol/L)	HbGp forms	R_g (\AA) ^a	R_g (\AA) ^b	D_{max} (\AA) ^a	$I(0)$ (a.u.) ^a
0.0	Oxy	107 \pm 1	108 \pm 10	300	0.047 \pm 0.002
2.0		106 \pm 1	109 \pm 8	300	0.021 \pm 0.001
3.0		107 \pm 1	109 \pm 9	300	0.025 \pm 0.002
4.0		120 \pm 2	124 \pm 14	450	0.006 \pm 0.002
5.0		215 \pm 5	175 \pm 12	680	0.004 \pm 0.001
5.5		225 \pm 6	175 \pm 30	750	0.005 \pm 0.002
0.0	Cyanomet	108 \pm 1	110 \pm 6	300	0.041 \pm 0.001
2.0		110 \pm 1	113 \pm 11	300	0.032 \pm 0.001
3.0		111 \pm 1	117 \pm 10	300	0.035 \pm 0.003
4.0		111 \pm 1	125 \pm 15	300	0.023 \pm 0.001
5.0		129 \pm 2	142 \pm 18	450	0.014 \pm 0.001
5.5		181 \pm 4	170 \pm 30	620	0.010 \pm 0.002

^a Parameters obtained by GNOM software. R_g is the radius of gyration, D_{max} the particle maximum dimension and $I(0)$ the scattering intensity at $q=0$.

^b Radius of gyration obtained by Guinier approximation.

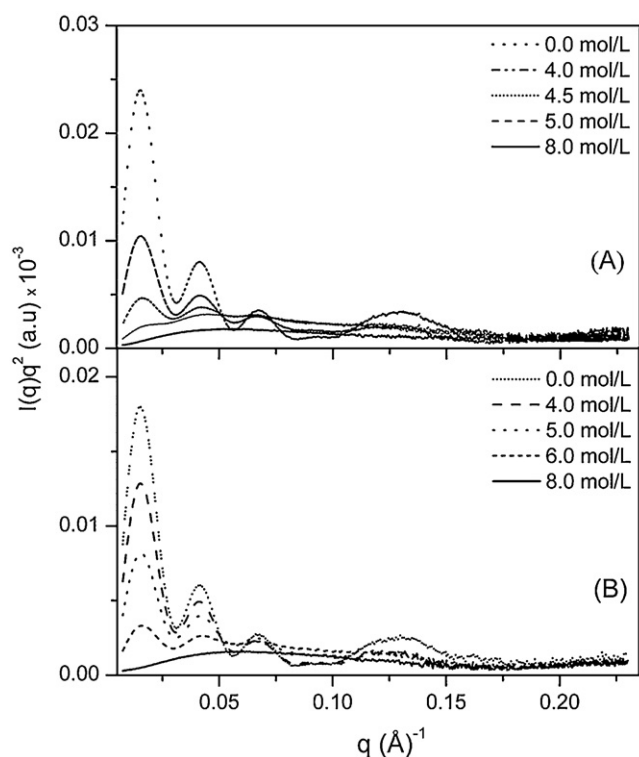


Fig. 4. Kratky plots for HbGp 3.0 mg/mL, in 30 mmol/L acetate-phosphate buffer at pH 7.0, in the presence of urea. (A) Oxy-HbGp and (B) cyanomet-HbGp.

protein solutions. At larger urea concentrations, an increase of the polydispersity index of the scattering particles size distributions is observed, associated to the dissociation/denaturation process. The results of SAXS and DLS experiments are quite consistent, confirming HbGp unfolding at higher urea concentrations, above 4.0 mol/L.

3.3. Unfolding model for HbGp in the presence of urea

Our previous study of HbGp, in the oxy- and cyanomet- forms, at pH 7.0, suggests that the HbGp oligomeric stoichiometry is similar to that proposed by Vinogradov [33] for HbLt. According to Vinogradov's model the structure of HbLt is composed of 12 protomers, composed by a globin dodecamer and three linker chains L , $(abcd)_3L_3$ [33]. A recent preliminary analysis of HbGp crystallographic structure, at 3.15 Å resolution [34], suggests that the stoichiometry, and the hierarchical levels of HbGp are the same as for HbLt. Thus, this model was used to describe the unfolding of HbGp, in the presence of urea. Moreover, recent results on the urea

effect upon three HbGp forms, monitored by several spectroscopic techniques [6], will be used for the description of this model.

Although the electronic density of the HbGp crystal is known, the crystallographic structure is not totally resolved, since only the polypeptide monomeric chain d has the primary sequence established. In the future, with the sequencing of all HbGp polypeptide chains, the crystallographic structure will be described in detail. Therefore, a complete description of the HbGp unfolding model, in the presence of urea, discussing the oligomeric interface in relation to the association equilibrium, the oligomeric intermediates and the oxygen cooperativity, will only be possible with the complete resolution of the crystallographic structure.

According to our experimental results, the HbGp unfolding process, in the presence of urea, is composed by two phases as shown in the schematic model in Fig. 5.

In the first one the oligomeric dissociation occurs, producing several smaller species, followed by the second one, where the dissociated species undergo denaturation. HbGp oligomeric dissociation, in the presence of urea, can be described by a model, where the whole protein $12x(abcd)_3L_3$ dissociates into the dodecamer $(abcd)_3$, at 2.0 mol/L of denaturant agent. At 3.0 mol/L, the dodecamer $(abcd)_3$ undergoes further partial dissociation into the tetramer $(abcd)$, Fig. 5). Increasing further the urea concentration to 4.0 mol/L, the tetramer $(abcd)$ starts to dissociate into the smaller species, trimer (abc) and monomer d . At concentrations, above 6.0 mol/L of urea, the dissociated species undergo denaturation. Our present AUC data shows clearly the partial HbGp oligomeric dissociation, at urea concentrations in the range from 2.0 to 4.0 mol/L. Previous work based on spectroscopic studies has shown that, in this concentration range, no significant changes in the protein secondary structure and heme groups are observed [6]. Thus, the possible intermediate state in the unfolding process is assigned to the partial oligomeric dissociation of the whole protein into several dissociated species in the equilibrium, maintaining its properties very close to the original native state.

Moreover, our present SAXS data show that the oxy- and cyanomet- forms undergo denaturation, at urea concentrations above 4.0 and 6.0 mol/L, respectively. The unfolding of the species is characterized by an increase of the values for D_{max} and R_g (Table 2). The decrease in the $I(0)$ values also suggests oligomeric dissociation. Besides, SAXS studies indicate a greater stability of the cyanomet-HbGp upon denaturation by urea, consistent with previous work, based on spectroscopic methods [6], and both HbGp oxidation forms follow the two-phases oligomeric dissociation model proposed in this paper (Fig. 5).

At this point it is worthy of mention the work on the subunits organization of HbLt linked to oxygen binding [14]. An important issue for HbGp future research is the correlation of structural data for subunits equilibrium in solution, under different conditions, with the main function which is oxygen binding and release. The study by Riggs mentioned above [14] suggested a special role for

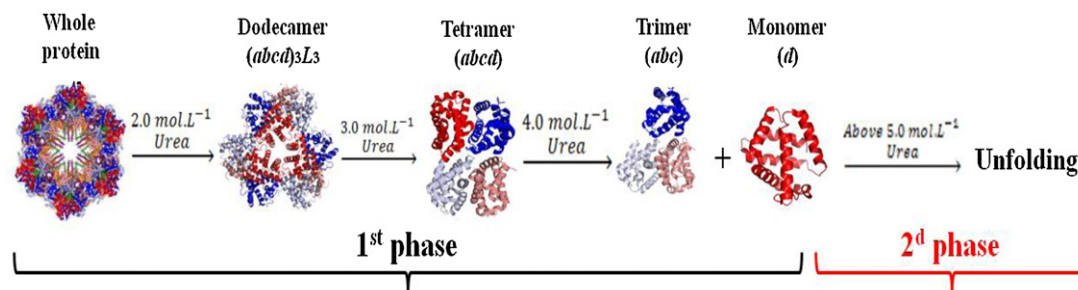


Fig. 5. Urea-induced oligomeric dissociation model for HbGp, at pH 7.0, based on the AUC and SAXS data. The crystallographic structure used in this scheme for the different subunits was adapted from the PDB bank under ID code 2GTL [7] and corresponds to the HbLt structure, which is similar to that of HbGp.

an octamer (dimer of tetramer, $(abcd)_2$), which was found incorrect in subsequent structural work by Royer group [35], which showed that the dodecamer is the main subunit in the oligomeric dissociation of the whole protein. Unfortunately, since no oxygenation data for HbGp subunits is presently available and since the crystal structure still needs some work before it will be available at high resolution, we cannot at the moment, to analyze in more detail the issue of subunits contacts. As noticed above, this is an interesting point for future research.

4. Conclusions

AUC and SAXS data analysis allowed the characterization of several species present in the equilibrium, and to evaluate the dissociation/denaturation processes in the presence of urea.

Our AUC data suggest that the species observed in the equilibrium are strongly dependent on the urea concentration. At low urea concentrations, below 4.0 mol/L, the larger species (whole protein and dodecamer) are predominant, and the increase of chaotropic agent induces the formation of smaller species in the solution, such as trimer (abc) and monomer (d). The $S_{20,w}^0$ and MM values obtained by AUC for all species are quite close to literature values reported for HbLt, as well as, to those found for HbGp, at alkaline pH. SAXS data show that the cyanomet-HbGp is more stable than oxy-HbGp, and both forms undergo unfolding above 4.0–5.0 mol/L of urea. These results are complementary to previous studies on the effect of urea upon three HbGp forms, monitored by various spectroscopic techniques [6], suggesting that HbGp undergoes partial oligomeric dissociation followed by denaturation at higher urea concentrations.

In summary, the HbGp unfolding process, in the presence of urea, is composed of two phases. The first one is associated to the protein oligomeric dissociation, while the second one to the species denaturation. Thus, the several dissociated species observed in solution, as a function of urea concentration, are assigned to the HbGp intermediate state in the unfolding process, observed from our previous spectroscopic study.

Acknowledgments

The authors are grateful to the Spectroscopy and Calorimetry Laboratory of the National Biosciences Laboratory (LNBio, Campinas, Brazil) and National Synchrotron Light Laboratory (LNLS, Campinas, Brazil) for making available the AUC and SAXS facilities used in this work. Thanks are due to the Brazilian agencies FAPESP, CNPq, and CAPES for partial financial support. F. A. O. Carvalho is a recipient of a Ph.D. grant from FAPESP (2009/17261-6). J.W.P. Carvalho is a recipient of a Ph.D. grant from FAPESP (2010/09719-0). M. Tabak is grateful to CNPq for a research grant. Thanks are also due to Mr. Ézer Biazin for efficient support in sample preparations.

References

- [1] S.N. Vinogradov, *Micron* 35 (2004) 127–129.
- [2] R.E. Weber, S.N. Vinogradov, *Physiological Reviews* 81 (2001) 569–628.
- [3] P.S. Santiago, J.W.P. Carvalho, M.M. Domingues, N.C. Santos, M. Tabak, *Biophysical Chemistry* 152 (2010) 128–138.
- [4] F.A.O. Carvalho, P.S. Santiago, J.C. Borges, M. Tabak, *International Journal of Biological Macromolecules* 48 (2011) 183–193.
- [5] P.S. Santiago, L.M. Moreira, E.V. Almeida, M. Tabak, *Biochimica et Biophysica Acta* 1770 (2007) 506–517.
- [6] F.A.O. Carvalho, P.S. Santiago, M. Tabak, *Archives of Biochemistry and Biophysics* 519 (2012) 46–58.
- [7] W.E. Royer, H. Zhu, T.A. Gorr, J.F. Flores, J.E. Knapp, *Journal of Biological Chemistry* 280 (2005) 27477–27480.
- [8] R.E. Hirsch, L.A. Jelicks, B.A. Wittenberg, D.K. Kaul, H.L. Shear, J.P. Harrington, *Artificial Cell Blood Substitute* 25 (1997) 429–444.
- [9] M. Rousselot, E. Delpy, R.C. Drieu La, V. Lagente, R. Pirow, J.F. Rees, A. Hagege, D. Le Guen, S. Hourdez, F. Zal, *Biotechnology Journal* 1 (2006) 333–345.
- [10] T. Harnois, M. Rousselot, H. Rogniaux, F. Zal, *Artificial Cell Blood Substitute* 37 (2009) 106–116.
- [11] F.A.O. Carvalho, P.S. Santiago, J.C. Borges, M. Tabak, *Analytical Biochemistry* 385 (2008) 257–263.
- [12] W.E. Royer, K. Strand, M. van Heel, W.A. Hendrickson, *Proceedings of the National Academy of Science of the United States of America* 97 (2000) 7107–7111.
- [13] M.S. Oliveira, L.M. Moreira, M. Tabak, *International Journal of Biological Macromolecules* 40 (2007) 429–436.
- [14] K. Fushitani, A.F. Riggs, *Journal of Biological Chemistry* 266 (1991) 10275–10281.
- [15] P.S. Santiago, F. Moura, L.M. Moreira, M.M. Domingues, N.C. Santos, M. Tabak, *Biophysical Journal* 94 (2008) 2228–2240.
- [16] J.W.P. Carvalho, P.S. Santiago, T. Batista, C.E.G. Salmon, L.R.S. Barbosa, R. Itri, M. Tabak, *Biophysical Chemistry* 163–164 (2012) 44–55.
- [17] A.L. Poli, L.M. Moreira, M. Tabak, H. Imasato, *Colloids and Surface B* 52 (2006) 96–104.
- [18] S.C.M. Agostinho, M.H. Tinto, J.R. Perussi, M. Tabak, H. Imasato, *Comparative Biochemistry and Physiology* 118A (1998) 171–181.
- [19] C.N. Pace, *Methods in Enzymology* 31 (1986) 266–280.
- [20] T.M. Laue, *Current Opinion in Structural Biology* 11 (2001) 579–583.
- [21] J. Lebowitz, M.S. Lewis, P. Schuck, *Protein Science* 11 (2002) 2067–2079.
- [22] P. Schuck, *Biophysical Journal* 78 (2000) 1606–1619.
- [23] P. Schuck, M.A. Perugini, N.R. Gonzales, G.J. Howlett, D. Schubert, *Biophysical Journal* 82 (2002) 1096–1111.
- [24] J. Vistica, J. Dam, A. Balbo, E. Yikilmaz, R.A. Mariuzza, T.A. Rouault, P. Schuck, *Analytical Biochemistry* 15 (2004) 234–256.
- [25] P. Schuck, *Analytical Biochemistry* 320 (2003) 104–124.
- [26] A. Guinier, G. Fournet, *Small Angle Scattering of X-ray*, Wiley, New York, 1955.
- [27] S.J. Perkins, R. Nan, K. Li, S. Khan, Y. Abe, *Methods* 54 (2011) 181–199.
- [28] H.D.T. Mertens, D.I. Svergun, *Journal of Structural Biology* 172 (2010) 128–141.
- [29] D.I. Svergun, *Journal of Applied Crystallography* 24 (1991) 485–492.
- [30] O. Glatter, O. Kratky, *Small Angle X-ray Scattering*, Academic Press, London, 1982.
- [31] A. Krebs, A.R. Kuchumov, P.K. Sharma, E.H. Braswell, P. Zipper, R.E. Weber, G. Chottard, S.N. Vinogradov, *Journal of Biological Chemistry* 271 (1996) 18695–18704.
- [32] F.A.O. Carvalho, J.W.P. Carvalho, P.S. Santiago, M. Tabak, *Process Biochemistry* 46 (2011) 2144–2151.
- [33] S.N. Vinogradov, S.D. Lugo, M.G. Mainwaring, O.H. Kapp, A.V. Crewe, *Proceedings of the National Academy of Science of the United States of America* 83 (1986) 8034–8038.
- [34] J.F.R. Bachega, L. Bleicher, E.R. Horjales, P.S. Santiago, R.C. Garratt, M. Tabak, *Journal of Synchrotron Radiation* 18 (2011) 24–28.
- [35] W.E. Royer, H. Sharma, K. Strand, J.E. Knapp, B. Bhyravhatla, *Structure* 14 (2006) 1167–1177.